

to the Curie temperature,  $T_c$ , as follows<sup>4</sup>:

$$kT_c \simeq 4\sqrt{2}J_{AB}\sigma_A\sigma_B - (4/3)J_{AA}\sigma_A^2 - 2J_{BB}\sigma_B^2, \\ \sigma_N^2 \equiv S_N(S_N+1). \quad (3)$$

As a first approximation, terms in  $J_{AA}$  and  $J_{BB}$  in Eqs. (2) and (3) may be considered negligible compared to terms in  $J_{AB}$ .<sup>7</sup> Then, setting  $S_A=2.5$  and  $S_B=2.25$  and the  $T^{\frac{1}{2}}$  term in Eq. (1) equal to the right-hand side of Eq. (2), we find that  $J_{AB} \simeq 5.15k$ , and from Eq. (3) that  $kT_c \simeq 45.2J_{AB}$ . The combination of these results gives  $T_c \simeq 235^\circ\text{K}$ , which is far below the directly measured value of  $848^\circ\text{K}$ .

It would be premature to attempt an explanation of this quantitative discrepancy in the light of only these preliminary results. We propose to extend these measurements to higher temperatures and to other ferrite crystals, and also study the effects of an external magnetic field on the spin-wave component of the specific heat.<sup>8</sup>

The author is very grateful to Professor H. Brooks and Professor N. Bloembergen for their encouragement in this work and to Mr. E. Weiss for his assistance in the measurements.

<sup>8</sup> J. S. Kouvel and H. Brooks, Technical Report 198, Cruft Laboratory, Harvard University, May 20, 1954 (unpublished).

## Components of the Thermodynamic Functions of Iron

R. J. WEISS AND K. J. TAUER\*

*Ordinance Materials Research Office, Watertown Arsenal, Watertown, Massachusetts*

(Received January 23, 1956)

The thermodynamic functions enthalpy, entropy, and free energy of alpha and gamma iron are determined from existing data. These functions are resolved into their magnetic, lattice, and electronic components on the basis of additivity of the respective specific heat components. The total magnetic entropy at the melting point approaches  $R \ln(2s+1)$ , where  $s$  is the unpaired spin per atom, indicating the validity of the method of separating specific heat components. A comparison plot of magnetic entropy *versus* temperature and saturation magnetization *versus* temperature qualitatively distinguishes the long- and short-range magnetic order. It is shown that the magnetic enthalpy at the melting point is of order  $kT_c$ , where  $T_c$  is the Curie temperature. It is further shown that in the absence of magnetic effects the  $\gamma$  lattice at absolute zero is more stable than the  $\alpha$  lattice by approximately 130 cal/mole. Finally, the components of the free energy are appropriately modified for the iron-rich FeMn alloy in order to determine the phase boundaries.

### INTRODUCTION

THE recent collation of Darken and Smith<sup>1</sup> probably contains the best values of the specific heat of  $\alpha$  iron and the deduced specific heat of  $\gamma$  iron. However, the existence of antiferromagnetism in  $\gamma$  iron with Néel temperature  $\sim 80^\circ\text{K}$  and moment  $\sim 0.57$  Bohr magnetons,<sup>2</sup> unknown to Darken and Smith, will modify their data. Their deduced specific heat curve for  $\gamma$  iron which depended on equating the entropies of the two phases from 0 to  $1353^\circ\text{K}$  is thus altered by virtue of the magnetic entropy of  $\gamma$  iron and results in a more realistic Debye temperature of  $335^\circ\text{K}$  rather than  $300^\circ\text{K}$  obtained by Darken and Smith. With the established specific heat curves of both the body-centered and face-centered iron phases, the enthalpies and entropies can then be determined as a function of temperature by graphical integration with careful attention to the maintenance of consistency with the known enthalpies and entropies at the transition

temperatures,  $1183^\circ\text{K}$  and  $1673^\circ\text{K}$ . Finally, the Gibbs free-energy functions as a function of temperature can then be established from the calculated enthalpy and entropy functions according to the definition  $G(T) \equiv H(T) - TS(T)$ .

Since the primary objective of these calculations is the application of the thermodynamic functions to iron-rich alloys, it was necessary in our case to analyze the total free energy functions into their component parts, i.e.,

$$G(T)_{\text{total}} = G(T)_{\text{magnetic}} + G(T)_{\text{lattice}} + G(T)_{\text{electronic}}.$$

These component parts were then appropriately modified in accordance with the known properties of the alloys to reconstruct the total free-energy functions for the alloy phases. This is an extension and correction of calculations previously reported by Zener.<sup>3</sup>

### COMPONENTS OF $\alpha$ IRON

The heat capacity data at low temperatures fit a Debye  $\theta$  of  $420^\circ\text{K}$ . The lattice specific heat at constant pressure was then calculated from the relation

<sup>3</sup> C. Zener, *J. Metals* **7**, 619 (1955).

\* Chemistry Department, Boston College, Chestnut Hill 67, Massachusetts.

<sup>1</sup> L. S. Darken and R. P. Smith, *Ind. & Eng. Chem.* **43**, 1815 (1951).

<sup>2</sup> Susceptibility and neutron diffraction data unpublished, Corliss, Hastings, and Weiss.

$C_p = C_v + \alpha_v^2 VT/\beta$  by the Nernst-Gruneisen relation  $C_p = C_v(1 + \gamma\alpha_v T)$ , where  $\gamma = \alpha_v V/C_v\beta$  was assumed independent of temperature. The coefficient of volume expansion  $\alpha_v$  was taken as triple the coefficient of linear expansion and the latter is obtained as a function of temperature from x-ray lattice parameter determinations of Basinski *et al.*<sup>4</sup> Finally, the total nonmagnetic specific heat at constant pressure was completed by adding the electronic specific heat term  $\gamma_{el}T$  where  $\gamma_{el} = 11.5 \times 10^{-4}$ . This yielded a calculated nonmagnetic specific heat equal to the measured value at the melting point and gave a  $\gamma_{el}$  value in good agreement with the low temperature value of  $\gamma_{el} = 12 \times 10^{-4}$ .<sup>5</sup> Manning's<sup>6</sup> calculations show that the density of states of body-centered iron at the Fermi surface does not vary appreciably with Fermi energy, so that qualitatively it is expected that  $\gamma_{el}$  does not vary appreciably with temperature. This conclusion is qualitative, since below the Curie temperature the electronic specific heat for each direction of spin is different and should be determined separately. The various specific heats are shown in Fig. 1.

The calculation of a total nonmagnetic specific heat allowed for the determination of the magnetic specific heat by difference between the measured  $C_p$  and the calculated lattice-plus-electronic  $C_p$ . Graphical integration of the  $C_p(T)$  curves then resulted in the enthalpy functions  $H_{total}(T)$ ,  $H_{magnetic}(T)$ ,  $H_{lattice}(T)$ , and  $H_{electronic}(T)$ . Since no additional information was gained by separation of the latter two, they were combined into a single function  $H_{nonmag}(T)$ . Graphical integration of the  $C_p(T)/T$  curves yielded the entropy functions  $S_{total}(T)$ ,  $S_{mag}(T)$ , and  $S_{nonmag}(T)$ . The magnetic and nonmagnetic functions,  $H(T)$  and  $S(T)$ , are tabulated in Table I. Several relations are worthy of emphasis.

(a) The limiting value of  $H_{mag}(T)$  is of order  $NkT_c$ ,<sup>7</sup> where  $T_c$  is the Curie temperature, i.e., the average thermal energy of Avogadro's number of particles at the Curie temperature. This may be considered the average energy required to uncouple the spin moments.

(b) The limiting value of  $S_{mag}(T)$  approaches  $R \ln(2s+1)$ , in which  $s$  is the number of unpaired spins; thus the measured entropy value approaches the statistical mechanical value for the disordering of  $N_{Avogadro}$  moments of strength  $2s$ . (This suggests a method of approximating the moment from specific heat data, as well as supporting the separation of magnetic and nonmagnetic components.)

(c) At the Curie temperature,  $T_c = 1043^\circ\text{K}$ , a significant fraction ( $\sim 35\%$ ) of the magnetic entropy

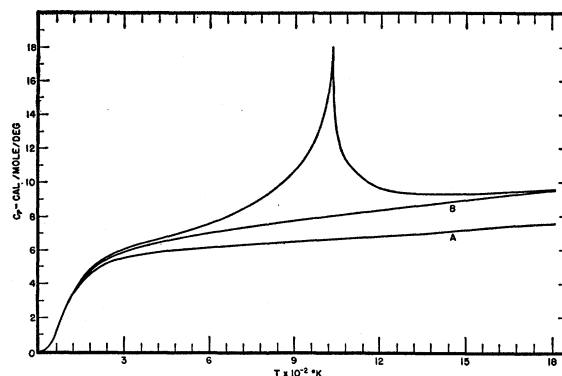


FIG. 1. Specific heat of  $\alpha$  (b.c.c.) Fe. Curve A is the calculated lattice specific heat for a Debye  $\theta = 420^\circ\text{K}$ . Curve B includes the electronic specific heat.

remains. Since the magnetization drops sharply to zero at  $T_c$ , the entropy remaining at  $T_c$  must be associated with short-range magnetic order. This is discussed more completely in a later paragraph.

#### COMPONENTS OF $\gamma$ IRON

The specific heat curve of  $\gamma$  Fe constructed by Darken and Smith was partly based on widely scattered measured data in the stable region of  $\gamma$  Fe but for the most part was adjusted to maintain thermodynamic consistency. We, however, have reconstructed the specific heat of  $\gamma$  iron in the following manner:

A Debye function with  $\theta = 335^\circ\text{K}$  was corrected for lattice expansion to  $C_p$ , again using x-ray lattice expansion data of Basinski *et al.*<sup>4</sup> The electronic specific heat was taken approximately from Manning and Greene<sup>6</sup> which indicated a density of states at the Fermi level of  $\frac{2}{3}$  that of  $\alpha$  iron. This gave a  $\gamma_{el}$  of  $8 \times 10^{-4}$ . The resulting specific heat curve agreed to within 2% of that chosen by Darken and Smith, except for low temperatures where the specific heat anomaly due to the

TABLE I. Magnetic and nonmagnetic enthalpy and entropy in cal/mole as a function of temperature for  $\alpha$  iron. The subscript zero refers to the values of the functions at absolute zero.  $(H_0)_{mag} = -2086$ ,  $(H_0)_{nonmag} = 0$ ,  $(S_0)_{mag} = 0$ ,  $(S_0)_{nonmag} = 0$ .

$T^\circ\text{K}$	$H_{mag}$	$H_{nonmag}$	$S_{mag}$	$S_{nonmag}$
400	-2063	1737	0.05	8.27
500	-2039	2353	0.09	9.81
600	-1999	3008	0.16	11.08
700	-1920	3744	0.28	12.26
800	-1796	4505	0.45	13.25
900	-1562	5226	0.72	14.09
1000	-1154	6048	1.16	14.89
1100	-638	6772	1.67	15.63
1200	-440	7614	1.84	16.39
1300	-334	8493	1.94	17.07
1400	-268	9352	1.99	17.72
1500	-221	10 245	2.02	18.28
1600	-188	11 052	2.04	18.88
1700	-171	11 745	2.05	19.47
1800	-161	12 373	2.06	20.04

<sup>4</sup> Z. S. Basinski *et al.* Proc. Roy. Soc. (London) **A229**, 459 (1955).

<sup>5</sup> R. Stoner, Acta Metallurgica **2**, 265 (1954).

<sup>6</sup> M. F. Manning, Phys. Rev. **63**, 190 (1943); J. B. Greene and M. F. Manning, Phys. Rev. **63**, 203 (1943).

<sup>7</sup> Hoffmann, Paskin, and Weiss, Bull. Am. Phys. Soc. Ser. II, **1**, 418 (1959).

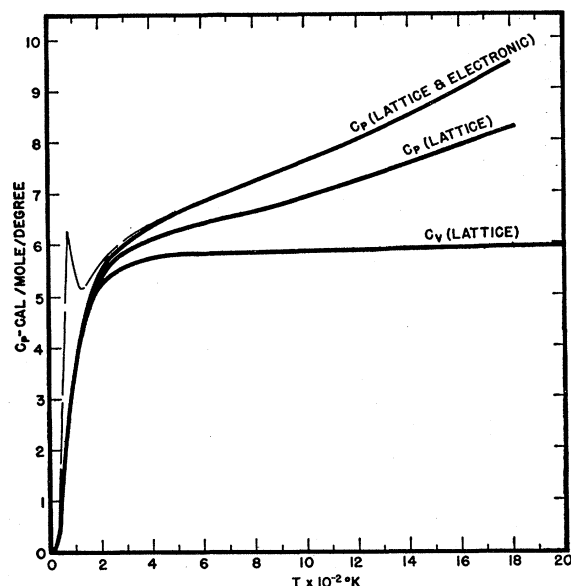


FIG. 2. The calculated specific heat components of  $\gamma$  (f.c.c.) Fe. antiferromagnetic Néel point<sup>8</sup> gave an appreciable magnetic enthalpy and entropy. It is precisely for this reason that our specific heat curve was fitted by a

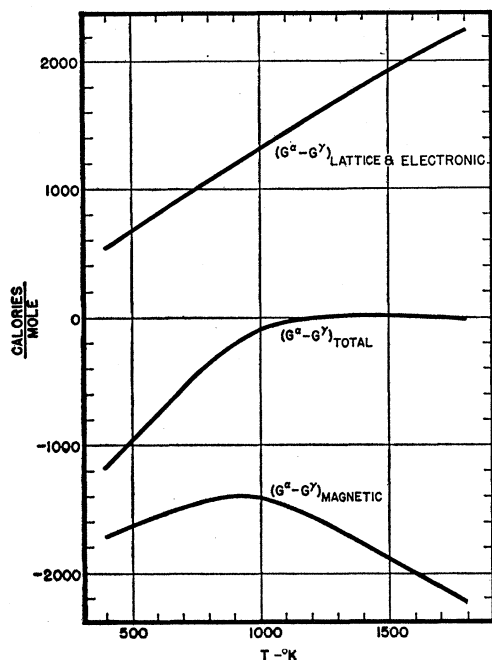


FIG. 3. The total free energy difference of  $\alpha$  and  $\gamma$  iron as a function of temperature together with its magnetic and non-magnetic components.

<sup>8</sup> Analysis of several magnetic lambda points (to be published) has substantiated the fact that the entropy/mole is essentially  $R \ln(2s+1)$  and the enthalpy/mole is of order  $RT_c$ . A similar analysis for  $\beta$  brass revealed the entropy, as determined from specific heat, and long range order as measured from x-ray super lattice intensity to be similarly related. Here too, an appreciable fraction of short-range order entropy persists above the critical temperature.

characteristic temperature of 335°K rather than the anomalously low value (compare neighboring f.c.c. elements) of 300°K indicated by the Darken and Smith curve. Thermodynamic consistency from the Third Law required the entropy difference ( $S^\alpha - S^\gamma$ ) from 0°K to 1353°K to be zero. With the magnetic entropy of  $\gamma$  iron added to the  $\gamma$  lattice entropy, such consistency was maintained. The several other conditions of thermodynamic consistency were also satisfied (see Darken and Smith<sup>1</sup>). Figure 2 is a plot of the calculated specific heat of  $\gamma$  iron with the magnetic anomaly included.

The total free-energy differences were then determined graphically from

$$(G^\alpha - G_0^\alpha)(T) - (G^\gamma - G_0^\gamma)(T) = \int_0^T (C_p^\alpha - C_p^\gamma) dT - T \int_0^T \frac{(C_p^\alpha - C_p^\gamma)}{T} dT, \quad (1)$$

TABLE II. Magnetic and nonmagnetic enthalpy and entropy in cal/mole as a function of temperature for  $\gamma$  iron. The subscript zero refers to the value of the function at absolute zero.  $(H_0)_{\text{mag}} = -160$ ,  $(H_0)_{\text{nonmag}} = -130$ ,  $(S_0)_{\text{mag}} = 0$ ,  $(S_0)_{\text{nonmag}} = 0$ .

$T^\circ\text{K}$	$H_{\text{mag}}$	$H_{\text{nonmag}}$	$S_{\text{mag}}$	$S_{\text{nonmag}}$
400	0	1727.5	0.91	9.60
500	0	2332.5	0.91	11.12
600	0	2982.5	0.91	12.37
700	0	3698.8	0.91	13.50
800	0	4421.6	0.91	14.47
900	0	5113.6	0.91	15.27
1000	0	5896.6	0.91	16.03
1100	0	6569.6	0.91	16.75
1200	0	7365.0	0.91	17.50
1300	0	8205.0	0.91	18.15
1400	0	9040	0.91	18.78
1500	0	9917	0.91	19.33
1600	0	10 711	0.91	19.92
1700	0	11 390	0.91	20.51
1800	0	12 015	0.91	21.07

where the subscript zero refers to the zero-point free energies and can be represented by

$$(G_0^\alpha)_{\text{total}} = (G_0^\alpha)_{\text{nonmag}} + (G_0^\alpha)_{\text{magnetic}}. \quad (2)$$

$(G_0^\alpha)_{\text{nonmag}}$  is taken as zero for all calculations (reference level) and

$$(G_0^\alpha)_{\text{mag}} = -RT_c = -2086 \text{ cal/mole}, \quad (3)$$

where the unmagnetized state at absolute zero is taken as zero.  $(G_0^\gamma)$  can similarly be factored and we then obtain

$$(G_0^\alpha - G_0^\gamma)_{\text{total}} = (-2086) - [-160 + (G_0)_{\text{nonmag}}] = -1926 \text{ cal/mole} - (G_0^\gamma)_{\text{nonmag}}. \quad (4)$$

The unknown quantity,  $(G_0^\gamma)_{\text{nonmag}}$ , was determined by matching free energies at the transition points 1183°K and 1673°K. This gave a value of  $(G_0^\gamma)$  equal to -130 cal/mole, i.e., neglecting magnetic effects, the  $\gamma$  lattice (f.c.c.) at 0°K is stable by 130 cal/mole

with respect to the  $\alpha$  lattice (b.c.c.). The magnetic and nonmagnetic functions  $H(T)$  and  $S(T)$  are tabulated in Table II.

Figure 3 is a plot of  $(G^\alpha - G^\gamma)$ . These values are also tabulated in Table III and compared to those of Darken and Smith. Included in Fig. 3 are the lattice (including electronic) and magnetic free energy components. It is apparent that the magnetic free energy, as pointed out by Zener, plays a decisive role in determining the relative stability of the two phases.

It can be seen from Table I that an appreciable fraction of the magnetic entropy remains above the Curie temperature. The Curie temperature, as indicated by a curve of magnetization *versus* temperature, marks the disappearance of long-range magnetic order and one is therefore left with some measure of the short-range magnetic order. Figure 4 shows a comparison of the experimental magnetization curve and the magnetic

TABLE III. Total free energy difference in calories per mole as a function of temperature of  $\alpha$  and  $\gamma$  iron.

	Darken and Smith	$(G^\alpha - G^\gamma)$ present work
400	-1110	-1178.5
500	-886	-965.5
600	-690	-752.5
700	-504	-553.8
800	-327	-351.6
900	-188	-218.6
1000	-76	-113.6
1100	-20.1	-40.6
1183	0	0
1200	2.6	2.4
1300	13.4	12.8
1400	16.1	16.0
1500	13.3	13.0
1600	6.6	8.3
1673	0	0
1700	-2.7	-1.8
1800	-13.3	-15.7

entropy change both normalized to unity. This clearly shows that at least up to temperatures close to the Curie point the major entropy change is qualitatively associated with the decrease in long-range order.<sup>9</sup> Experimental evidence of short range order above the Curie temperature has been collected by Shull<sup>10</sup> from neutron diffraction experiments and indicates presence of short-range order at least up to the transition temperature of 1183°K. However, a direct comparison of short-range order from neutron diffraction experiments with the remaining magnetic entropy of Fig. 4 requires a specific model and no attempt has been made to effect such a comparison.

### $H(S)$ CURVES

In order to extend these thermodynamic relations to iron-rich alloys with known Curie or Néel temperatures

<sup>9</sup> Note added in proof.—At temperatures up to  $T_c/3$  it can be shown from spin wave theory that both functions plotted in Fig. 4 can be given as  $1 - AT^3$  where  $A$  is a constant.

<sup>10</sup> C. G. Shull (to be published).

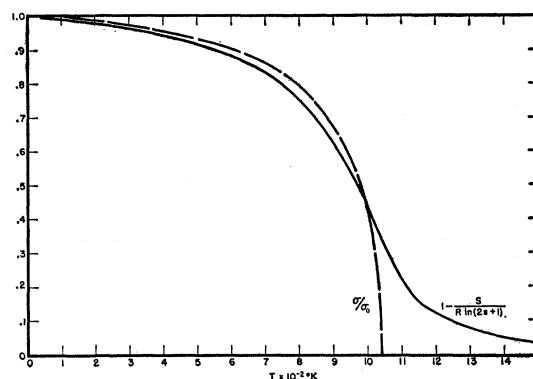


FIG. 4. The reduced saturation magnetization of  $\alpha$  iron as a function of temperature together with the reduced magnetic entropy change of  $\alpha$  iron indicating the close relation between entropy and long-range order at temperatures below the Curie temperature.

and Bohr magneton numbers, but unknown specific heat data, a study was made of many magnetic lambda points. In each of these cases the measured specific heat data were analyzed similar to that of  $\alpha$  iron and the anomalous specific heat determined. From this the magnetic  $H(T)$  and  $S(T)$  functions were obtained, and most conveniently plotted as  $H$  *versus*  $S$  curves. The  $\alpha$  iron curve, Fig. 5, was found to be typical. These curves have the following general features:

- The tangent at any point,  $dH/dS$ , is the temperature.
- The intercept with the  $H$ -axis of any tangent to the curve is the magnetic free energy for that temperature.

The specific similar features noted were as follows:

- Approximately 70–85% of the available magnetic entropy and about 60–75% of the available magnetic enthalpy are liberated up to the Curie or Néel temperature.
- The terminus of the curve is at the point  $H \cong RT_c$  and  $S = R \ln(2s+1)$ , consistent with our finding for  $\alpha$  iron.

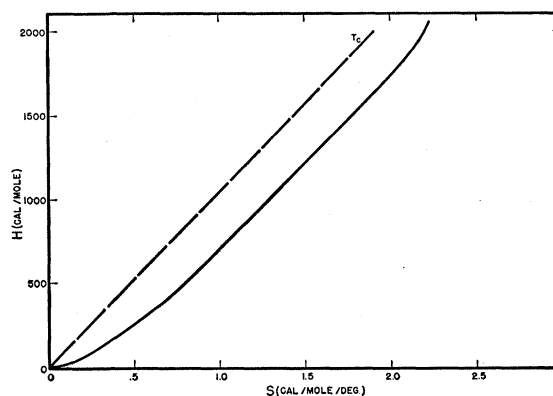


FIG. 5. The magnetic enthalpy *versus* entropy curve of  $\alpha$  iron.

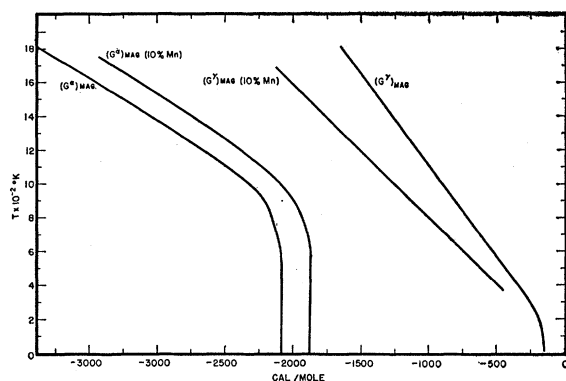


FIG. 6. The magnetic free energy of  $\alpha$  and  $\gamma$  iron and a 10% Mn  $\alpha$  and  $\gamma$  alloy.

(3) In the case of transition metals and alloys with similar crystal structure, a simple technique of deducing the magnetic  $H$  versus  $S$  curve involved a contraction of the  $H$  scale by the ratio of the Curie temperatures and the  $S$  scale by the ratio of the logarithms  $(2s+1)$ , since the Curie temperatures were found to be proportional to the  $\ln(2s+1)$ . This relationship is illustrated in Table IV for many alloys, where the ratio of the observed and calculated Curie temperatures to  $\ln(2s+1)$  are plotted. This ratio for f.c.c. alloys was 1.5 times the ratio for b.c.c. alloys which is merely the ratio of the number of nearest neighbors.

These relations enable one to construct a good approximation to the magnetic  $H$  versus  $S$  curve for any transition metal with known Curie or Néel temperature and Bohr magneton number. From this, the magnetic free energy versus temperature and the anomalous specific heat versus temperature can be obtained.

#### EXTENSION TO IRON-RICH ALLOYS

An extension of the above thermodynamic consideration was made to the iron rich region of the iron manganese system. This system was chosen for several reasons:

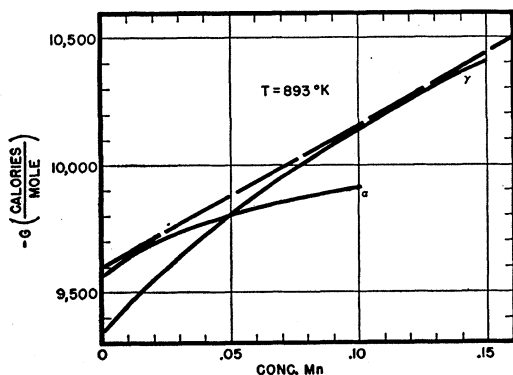


FIG. 7. The free energy versus concentration of Mn of  $\alpha$  and  $\gamma$  alloy at 893°K. The common tangents denote the concentrations of equal chemical potentials.

TABLE IV. The ratio of Curie temperature in degrees Kelvin to  $\ln(2s+1)$ , where  $2s$  is the spin for ferromagnetic elements and alloys of the first transition group.<sup>a</sup>

Face-centered cubic	Substance	Ratio $T_c$		Body-centered cubic	Substance	Ratio $T_c$	
		$\ln(2s+1)$				$\ln(2s+1)$	
NiCo	0% Ni	1400		FeCr	30% Fe	875	
	20% Ni	1410			50% Fe	910	
	50% Ni	1420			70% Fe	882	
	75% Ni	1380			100% Fe	900	
	100% Ni	1330			FeCo	85%	970
					FeAl	70%	970
NiCu	50% Ni	1270		FeMn	84%	895	
NiCr	90% Ni	1400					
NiMo	95.73% Ni	1300					
NiSi	91.4% Ni	1240					
NiZn	88.1% Ni	1460					
NiW	85% Ni	1420					
CoMo	95% Co	1320					
CoCr	95% Co	1350					
		Av = 1360 ± 50					

Av = 1360  $\pm$  50

<sup>a</sup> All data taken from R. Bozorth, *Ferromagnetism* (D. Van Nostrand Company, New York, 1951).

(a) Data are available giving the effect of Mn on both Curie temperature and Bohr magneton number for both  $\alpha$  phase<sup>11</sup> and  $\gamma$  phase.<sup>12</sup> Table V lists these effects.

(b) The Debye temperatures of iron and manganese are sufficiently similar so that the change in lattice free energy is expected to be small compared to magnetic free energy and can be neglected.

(c) There is no evidence for atomic ordering in the alloys so that the thermodynamics of ideal solutions are sufficient.

Since equilibrium in a heterogeneous system is governed by equal chemical potentials of the various components of all phases in equilibrium, the determination of phase diagrams reduces to the problem of the determination of chemical potentials. This is most conveniently done here, by graphically determining the common tangent to the free energy versus concentration curves for the  $\alpha$  and  $\gamma$  phases.<sup>13</sup> In the iron-manganese system these curves were determined in the following manner:

(a) The lattice free energies for both  $\alpha$  and  $\gamma$  phases were assumed independent of manganese concentrations and therefore the pure iron functions were corrected only for the entropy of mixing. This is equivalent to the assumption that over the concentration range of interest (0–30% Mn) the lattice characteristic tem-

TABLE V. Change of Curie temperature and Bohr magneton number of  $\alpha$  and  $\gamma$  iron with addition of Mn.

	$\Delta T_c$ (degrees)	$\Delta s$ (Bohr magnetons)
	$\Delta C$ (Mn)%	$\Delta C$ (Mn)%
$\alpha$ alloy	–10.6	–0.03
$\gamma$ alloy	+6.4	+0.02

<sup>11</sup> R. Bozorth, *Ferromagnetism* (D. Van Nostrand Company, New York, 1951), p. 235.

<sup>12</sup> Corliss, Hastings, and Weiss (to be published).

<sup>13</sup> L. S. Darken and R. W. Gurry, *Physical Chemistry of Metals* (McGraw-Hill Book Company, Inc., New York, 1953), p. 240.

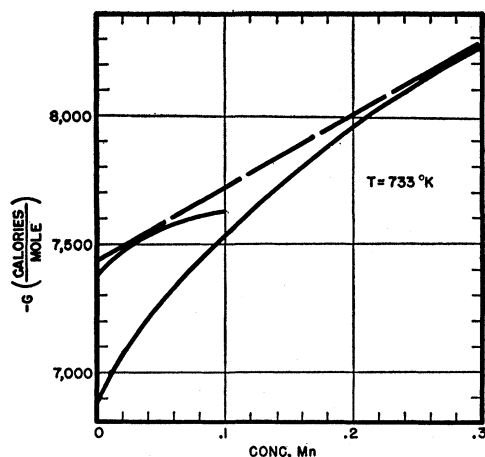


FIG. 8. The free energy versus concentration of Mn of  $\alpha$  and  $\gamma$  alloy at 733°K.

peratures do not change appreciably, nor do the lattice zero point energies change significantly.

(b) The magnetic free energy of the  $\alpha$  phase was determined by a reduction in scale of the magnetic  $H$  versus  $S$  curve of pure  $\alpha$  iron. The reduction was in the ratio of Curie temperatures for the  $H$  scale and of  $\ln(2s+1)$  for the  $s$  scale. This is illustrated for 10% Mn in Fig. 6.

(c) The magnetic free energy of the  $\gamma$  phase is simply  $[-RT \ln(2s+1)]$  since the phase boundaries were calculated only in the temperature region well above the Néel temperatures so that the spins are completely uncoupled. This also is illustrated for 10% Mn in Fig. 6.

These considerations enabled the calculation of the free energies as a function of concentration of Mn for the two phases and are shown in Figs. 7 and 8 for the temperatures 893°K and 733°K respectively. The common tangents shown, determined the phase boundaries. Figure 9 shows the experimental and calculated phase boundaries.

#### EXTENSION TO OTHER ALLOYS

Since no data are available on the effect of other alloy elements on the magnetic properties of the  $\gamma$  phase, it was not feasible to extend this analysis to other systems. However, the following general remarks are appropriate for future calculations when such data are available.

(a) In addition to the magnetic effects of the alloying elements one must know the change in Debye temperature as well as the change in the electronic specific heat term<sup>14</sup> and zero-point lattice free energy as a function of concentration. As the alloying and parent ele-

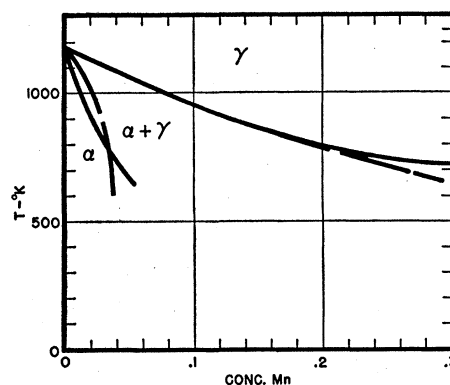


FIG. 9. The calculated and observed iron-rich Fe-Mn phase diagram. (Solid line calculated.)

ments become more removed in the periodic table, these factors will become more important and necessary. For example, the zero-point energies of elements below iron favor the  $\alpha$  phase (b.c.c.) while the elements above iron favor the  $\gamma$  phase (f.c.c.). It is estimated that for chromium this difference is of the order of 3500 cal/mole ( $\alpha$  stable) as compared to 130 cal/mole ( $\gamma$  stable) for iron.

(b) Any effects of atomic ordering will clearly vitiate the ideal entropy of mixing terms included in the analysis of Fe-Mn presented here.

(c) If the masses of the two elements in the alloy are very dissimilar, the optical branch of the frequency spectrum may add additional Einstein terms.

#### COMPARISON TO PREVIOUS WORK

While Zener<sup>3</sup> has correctly realized the importance of the magnetic free energy, we wish to make the following comments concerning his work. (1) The assumption that the nonmagnetic free energy difference of  $\alpha$  and  $\gamma$  iron is linear with temperature, assumes that the nonmagnetic specific heats are equal. This would only be correct if the coefficients of linear expansion and the electronic  $\gamma_{el}$  terms were identical. (They are not.) (2) No attempt is made to calculate chemical potentials which are the thermodynamically determining property. (3) Zener neglects entropy of mixing in his calculations as well as ordering effects. This is particularly serious for Fe-Al. (4) The effect of alloying elements is not merely to shift the magnetic free energy curve parallel to the temperature axis, but to change its shape since the change in Bohr magneton numbers alters its final slope. (5) The effect of alloying elements is not merely to shift the nonmagnetic free energy normal to the temperature axis, but rather involves all of the considerations discussed in the section "Extension to Other Alloys." (6) The use of the  $M_s$  (Martensite start) temperature is not thermodynamically acceptable as an equilibrium property.

<sup>14</sup> R. Smoluchowski and J. Koehler, Ann. Rev. Phys. Chem. 2, 187 (1941).